Lorentz Type Self-Bearing Motor using Halbach Magnets

Yohji Okada, Takuro Jinbu, Naoto Yamashiro, and Kouji Sagawa
Department of Mechanical Engineering,
Ibaraki University
4-12-1 Nakanarusawa, Hitachi 316-8511, Japan
y.okada@mx.ibaraki.ac.jp

I. Abstract

This paper proposes a 4-pole outer rotor type self-bearing motor which uses Lorentz force with Halbach magnet. It is expected to have good dynamic response and high levitation capability. For realizing high magnetic flux in airgap, Halbach magnet is used for the rotor. First, previous model of 8-pole motor is introduced and the associated problems are summarized. That is, the control forces for x and y directions were quite different and the levitation was unstable. For stable levitation, two sets of three phase coils were used and the system became complex. To overcome these problems, a new 4-pole and three segmented Halbach magnets are introduced. The fundamental principle is explained how the motor produces rotating torque and radial levitation forces. Finally, the motor is designed and fabricated. The levitated rotating test was carried out successfully. The top speed of 7400 [rpm] and the maximum motor efficiency of 72 [%] were recorded.

II. Introduction

For realizing high speed and maintenance free rotary machine, magnetic bearings have been gradually used[(1)]. Usually driving motor is installed between the two radial magnetic bearings. This construction causes long rotor shaft and low bending vibration.

Several types of self-bearing motors have been proposed which have combined functions of AC motor and magnetic bearings[(2)(3)]. However the standard self-bearing motor uses reluctance force to produce bearing force. Applying this technique to the permanent magnet (PM) type motor, thin PMs are requested which cause high manufacturing cost, weak PM strength and easy demagnetization[(4)].

To overcome these problems Lorentz type self-bearing motor is proposed which uses Lorentz force principle to produce both motoring torque and bearing forces[(4)(5)]. Lorentz type one can use thick PMs and free from the above problems. However the back yoke should be thick for strong magnetic circuit. The flux density produced by the radially magnetized PMs is apt to change stepwise flux causing bearing force fluctuation.

In this paper Halbach magnet is proposed for outer rotor type self-bearing motor. The ideal Halbach magnet requests constantly rotating magnetization which produces strong sinusoidal magnetic flux in one side and no flux in the other side[(6)]. First, previous model of 8-pole motor is introduced and the associated problems are summarized[(7)]. For overcome this problems, a new 4-pole and three segmented Halbach magnets are introduced. The fundamental principle is explained how the motor produces rotating torque and radial levitation forces. Then, the motor is designed and fabricated. The levitated rotating test was carried out successfully. The results obtained were discussed in details.

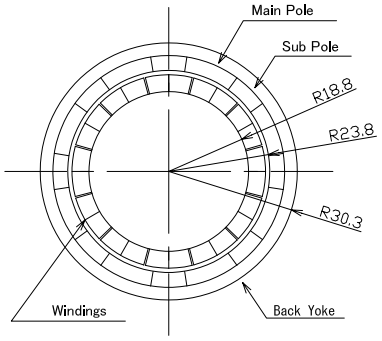

Fig. 1. Schematic of Experimental Setup

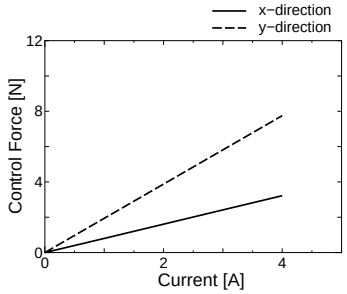

Fig. 2. Analytical Results

III. Problems with previous 8 pole motor

The schematic sectional diagram of 8 pole motor is shown in Fig. 1. The motor is outer rotor type and radial two directions are controlled actively while the axial and tilt directions rely on passive stability. The levitation and rotation control coils were wound 96 and 48 turns, respectively. Both of them are non-salient wound coils. They are separated $\frac{\pi}{6}$ apart to improve the coil space efficiency.

We could not succeed for levitated rotation. The main reason is the levitation force fluctuation as the relative angle between the rotor and stator. The levitation forces for x and y directions are shown in Fig. 2 when the rotor

TABLE I

DEFINITION OF VARIABLES

A	Magnitude of Motoring Current
B	Flux Magnitude by Permanent Magnets
C	Magnitude of Levitation Current
l	Effective Length of Windings
r	Diameter of Rotor
t	Time
θ	Coordinate Angle
ψ	Phase of Motoring Current
ϕ	Phase of Levitation Current
ω	Electric Frequency

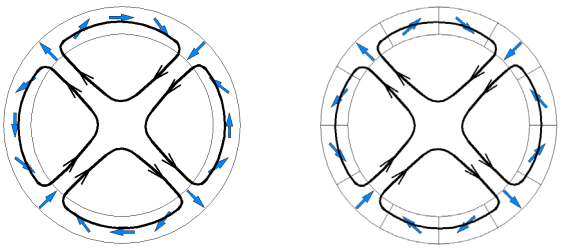

Fig. 3. Ideal and 3 Segmented Halbach Magnet

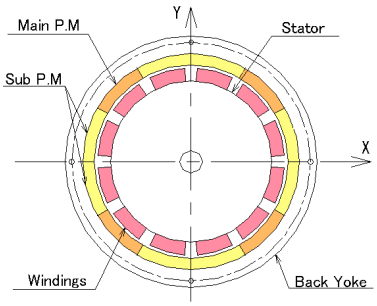

Fig. 4. Analytical Model of 4 Pole 3 Seg. Motor

TABLE II

ANALYTICAL PARAMETERS

Stator Material	Silicon Sheet
Outer Dia. of Stator	50 [mm]
Permanent Magnet	Neomax-38H
Segment Ratio	1:1
Thickness of PM	3.5 [mm]
Thickness of Backyoke	5.5 [mm]
Coil Height	4 [mm]
Coil Width	22.5 [deg]
Airgap with Coil	5 [mm]

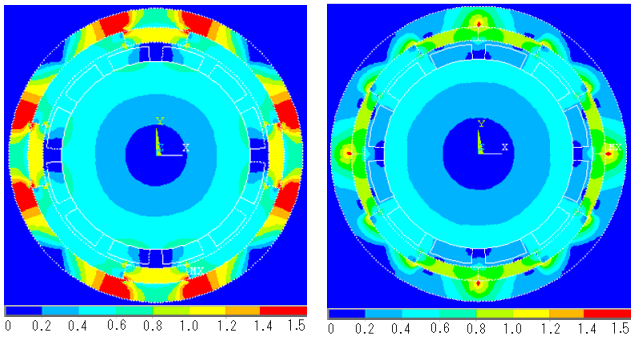

Fig. 5. Flux Density Distributions of 4 Pole 2 Seg. and 3 Seg. Magnets

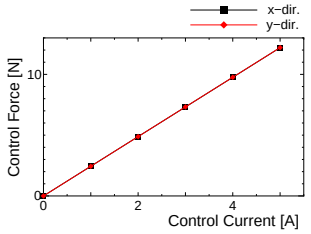

Fig. 6. Calculated Control Forces

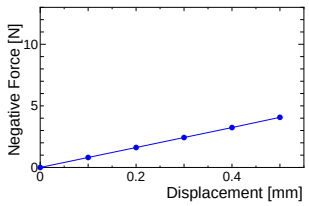

Fig. 7. Calculated Negative Stiffness

and stator positions are in Fig. 1. The levitation control is developed on the assumption of sinusoidal distributed radial flux. Due to the wide airgap, however, the flux path has the circumferential component which affects adversely to the constant levitation force, as shown in Fig. 2 [7].

In the previous research we modified the control circuit to use the rotation coils as the sub levitation coils to reduce the levitation force fluctuation. Then we could succeed the levitated rotation. But the control circuit became complex and the force and torque were not so strong than we expected [7].

IV. 4 POLE MOTOR

The outer rotor type 8 pole motor has the merit that the coil ends are not overlapped, but the flux path has strong circumferential component causing the previously mentioned troubles. In this section we propose a new 4 pole Lorentz motor which has wider magnetic pole length. This is expected to reduce the levitation force fluctuation drastically and to have the stronger torque and bearing forces.

A. Theoretical Background

Suppose that the rotor PMs produce the following sinusoidally distributed magnetic flux in the airgap,

$$B_g = B\sin(\omega t + 2\theta) \tag{1}$$

where the symbols used are listed in Table I.

The following three phase currents are assumed to flow in each motoring coils.

$$\begin{aligned} I_{U_m} &= A\cos(\omega t + \psi) \\ I_{V_m} &= A\cos(\omega t + \frac{2}{3}\pi + \psi) \\ I_{W_m} &= A\cos(\omega t + \frac{4}{3}\pi + \psi) \end{aligned} \tag{2}$$

The entry and return coils are assumed to be $\frac{\pi}{4}$ part, the half of the circumferential coil distribution can be expressed using the Dirac delta function as,

$$\begin{aligned} i_m &= I_{U_m}\left[\delta(\theta + \frac{\pi}{4}) - \delta(\theta - \frac{\pi}{4})\right] \\ &+ I_{W_m}\left[\delta(\theta - \frac{\pi}{12}) - \delta(\theta - \frac{7}{12}\pi)\right] \\ &+ I_{V_m}\left[\delta(\theta - \frac{5}{12}\pi) - \delta(\theta - \frac{11}{12}\pi)\right] \end{aligned} \tag{3}$$

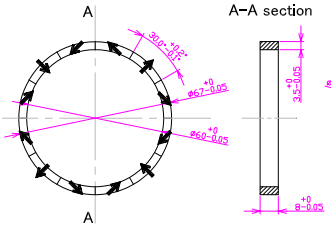

Fig. 8. Schematic of Designed PM

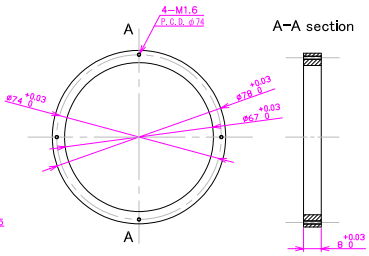

Fig. 9. Schematic of Designed Back Yoke

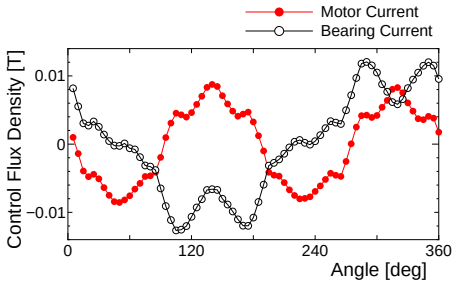

Fig. 10. Measured Flux Density Distribution

TABLE III
SPECIFICATIONS OF WINDINGS

Number of Coils	6
Coil Diameter	ϕ 0.5 [mm]
Turns	96
Effective Length	8 [mm]
Total Ef. Length	0.768 [m]

TABLE IV
MEASURED INDUCTANCES

Phase	120 [Hz]	1 [Hz]
U	0.808 [H]	0.795 [H]
V	0.807 [H]	0.795 [H]
W	0.820 [H]	0.808 [H]
−U	0.813 [H]	0.793 [H]
−V	0.815 [H]	0.799 [H]
−W	0.826 [H]	0.832 [H]

From the BLI law, the torque can be expressed as,

$$\begin{aligned} T &= 2rl\int_0^{\pi} B_g i_m d\theta \\ &= 2rlAB\Big[2\cos(\omega t+\psi)\cos(\omega t) \\ &\quad +2\cos(\omega t+\frac{2}{3}\pi+\psi)\cos(\omega t+\frac{2}{3}\pi) \\ &\quad +2\cos(\omega t+\frac{4}{3}\pi+\psi)\cos(\omega t+\frac{4}{3}\pi)\Big] \\ &= 6rlAB\cos\psi \end{aligned} \tag{4}$$

This means that the motor torque can be controlled similar to the PM synchronous motor either by changing the current amplitude A or phase ψ.

Next, let us consider the levitation control. For this purpose we use the following three phase current.

$$\begin{aligned} I_{U_b} &= C\cos(\omega t+\phi) \\ I_{V_b} &= C\cos(\omega t+\frac{2}{3}\pi+\phi) \\ I_{W_b} &= C\cos(\omega t+\frac{4}{3}\pi+\phi) \end{aligned} \tag{5}$$

The current distribution is expressed similarly using the Dirac delta function as,

$$\begin{aligned} i_b &= I_{U_b}[\delta(\theta+\frac{\pi}{4})-\delta(\theta-\frac{\pi}{4}) \\ &\quad -\delta(\theta-\frac{3}{4}\pi)+\delta(\theta-\frac{5}{4}\pi)] \\ &+ I_{V_b}[-\delta(\theta-\frac{\pi}{12})+\delta(\theta-\frac{7}{12}\pi) \\ &\quad +\delta(\theta-\frac{13}{12}\pi)-\delta(\theta-\frac{19}{12}\pi)] \\ &+ I_{W_b}[\delta(\theta-\frac{5}{12}\pi)-\delta(\theta-\frac{11}{12}\pi) \\ &\quad -\delta(\theta-\frac{17}{12}\pi)+\delta(\theta+\frac{\pi}{12})] \end{aligned} \tag{6}$$

Applying the BLI law, we have the following bearing force for y and x directions,

[$y-$directional force]

$$\begin{aligned} F_y &= \int_0^{2\pi} B_g i_b l\cos(\theta)d\theta \\ &= \frac{3\sqrt{2}}{2}BCl\cos(\phi-\frac{\pi}{4}) \end{aligned} \tag{7}$$

[$x-$directional force]

$$\begin{aligned} F_x &= -\int_0^{2\pi} B_g i_b l\sin(\theta)d\theta \\ &= -\frac{3\sqrt{2}}{2}BCl\sin(\phi-\frac{\pi}{4}) \end{aligned} \tag{8}$$

From Eqs. (7) and (8), the levitation can be controlled independently from the motoring control. Also the x and y directions are controlled individually.

B. Design of Halbach Magnet

Schematic of ideal and 3 segmented Halbach magnets is shown in Fig. 3. Previously we used 2 segmented 8 pole magnet. But we used 3 segmented 4 pole magnet for reducing the back yoke thickness.

The analytical model for finite element analysis is shown in Fig. 4 and the parameters are listed in Table II. The inner stator has the diameter of 50 [mm] and the thickness of 8 [mm] with the silicon steel sheet. The outer rotor and the permanent magnets are designed using the FEM package ANSYS. The flux density distributions of 2 and 3 segmented magnets are shown in Fig. 5. The back yoke flux has the saturated part in case of 2 segment while the 3 segment results have better flux distribution. Then we decided to use the 3 segmented Halbach magnets.

TABLE V

PHYSICAL PARAMETERS OF PERMANENT MAGNET

Item		Value
Residual Magnetization	B_r	1.245 [T]
Initial Coercive Force	iH_c	1352 [kA/m]
Coercive Force	bH_c	959 [kA/m]
Maximum Energy Product	$(BH)_{max}$	302.5 [kJ/m^3]

TABLE VI

DESIGN PARAMETERS OF ROTOR

Item	value	Item	value
Outer Diameter	78 [mm]	Thickness of PM	3.5 [mm]
Inner Diameter	60 [mm]	Pole	4
Thickness	8 [mm]	Rotor Mass	110 [g]

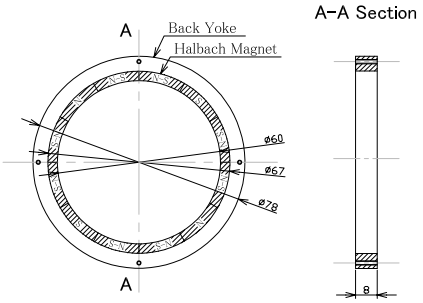

Fig. 11. Schematic of Rotor

C. Control Force and Negative Stiffness

The calculated control force and negative stiffness force are shown in Figs. 6 and 7. The forces are almost the same for x and y directions and indicate enough strong values compared with the case of 8 pole motor. The negative force is about 3.5 [N] at 0.4 [mm] displacement while the control force is about 10.5 [N] at 4 [A]. Hence this value is considered strong enough to control the motor.

V. LEVITATED ROTATING TEST

From the FEM analysis we designed and fabricated the experimental setup.

A. Experimental Setup

Figure 8 shows designed PM and Fig. 9 indicates back-yoke used. The sub magnets should be magnetized 60^o direction, hence it requires a special magnetization tools.

Specification of the stator coils is shown in Table III and the measured inductances are shown in Table IV. The inductances are almost the same values. The flux distribution made by motor coils and levitation coils are shown in Fig. 10. They are 4 pole and 2 pole fluxes as expected.

The rotor is fabricated according to the design mentioned previously. One rotor pole is composed of three PMs and the PM characteristics is shown in Table V. Schematic of the rotor is shown in Fig. 11 and the parameters are listed in Table VI. The calculated rotor weight is about 110 [g] and inclination moment of inertia is about $J = 8.9 \times 10^{-5}$ [kgm^2], respectively. The measured flux density of the rotor PMs with stator is shown in Fig. 12. This is measured using the Gauss meter (Lake Shore 421) at 120 points with 3° each. This indicates nearly sinusoidal distribution with the maximum value about 0.41 [T]. We could not recognize any flux leakage outside the rotor.

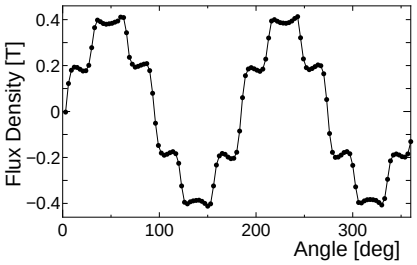

Fig. 12. Flux Density Distribution by Rotor Magnet

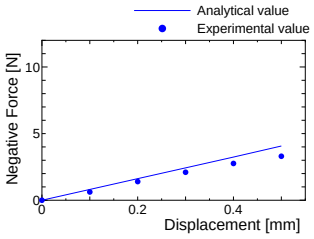

Fig. 13. Measured Negative Force

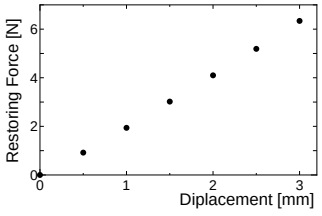

Fig. 14. Measured Restoring Force

Figure 13 indicates the measured negative stiffness using the digital force gauge. The forces are measured from the center to 0.5 [mm] at the step of 0.1 [mm] eccentric. From this measurement we estimate the negative stiffness of K_n=6.2 [kN/m].

The axial and tilt of the motor rely on passive stability. The axial restoring force is measured similarly as shown in Fig. 14. Also we estimate the restoring force factor as K_z=2.13 [kN/m] for axial and $K_{x\theta}$=0.9 [Nm/rad] for tilt directions. From these values we calculate the resonant frequency of axial and tilt as 958 and 1327 [rpm], respectively.

The photo of self-bearing motor is shown in Fig. 15. This is used to measure the previous data for confirming the proposed technique.

B. Control System

Schematic of control system is shown in Fig. 16. The system is composed of the designed motor, gap sensor (Shinkawa, VC-202N), dSPACE (DS-1104) and linear power amplifier (Apex PA-12, Max $\pm$24 [V] 4 [A]). The measured x and y displacements are put into DSP via A/D converters to calculate the PID control signals. They are converter to each coil current through 2-3 phase converter and added the motoring coil currents. Finally they are put out to the power amplifiers via D/A converters.

C. Control Force and Torque

The levitation force is measured as shown in Fig. 17, the force gain of 2.5 [N/A] is obtained. Figures 18 and 19 show the measured maximum torque at the motoring current of 1, 1.5 and 2 [A], respectively. The measured data are the phase difference from $0^\circ$to maximum 90° at each 5°.

The measured data are lower than the expected dashed lines. However, They are relatively linear and have the

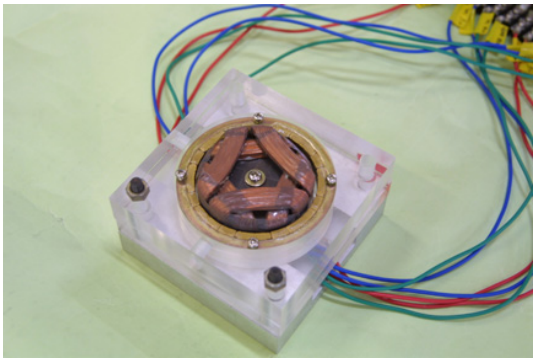

Fig. 15. Experimental Setup of the Motor

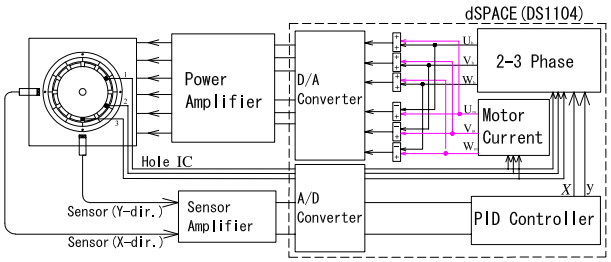

Fig. 16. Control System

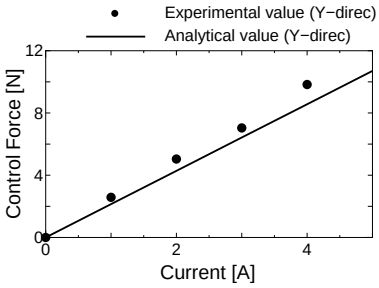

Fig. 17. Control Force

torque factor about 0.04 [Nm/A]. The reason of the lower measured data is considered due to the flux leakage in three dimensions.

D. Motor Characteristics

The motor characteristics is measured by measuring the dynamic torque and motor efficiency. The dynamic torque is measured by using the hysterisys brake. The maximum torque about 0.04 [Nm] is recorded at non-rotating speed and decreasing according to the rotating speed at the motor current of 1 [A]. This is the typical synchronous motor characteristics. The motor efficiency is measured using the output power versus input power as shown in Fig. 21. The maximum efficiency is recorded as 72 [%] at the speed of about 3500 [rpm].

E. Impulse Response

Impulse response test is carried out when the rotor is stably levitated. The control parameters are listed in Table VII. The rotor is excited about 0.3 [mm] displacement either for x or y direction by adding the 0.1 [ms] narrow pulse signal from the computer and recording the corresponding responses. The results are shown in Figs. 22 and 23. The both disturbances are decayed within 0.02 [sec]

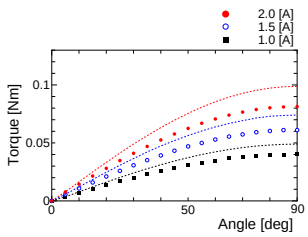

Fig. 18. Motoring Torque

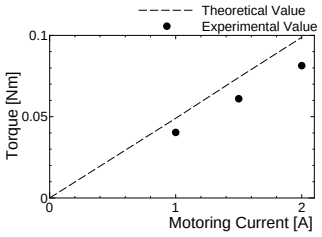

Fig. 19. Maximum Motoring Torque

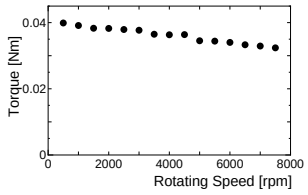

Fig. 20. Dynamic Torque versus Rotating Speed

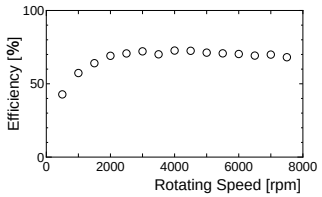

Fig. 21. Motor Efficiency

and the mutual influence is not recognized. This means that the dynamic stability is well controlled by the proposed controller.

F. Frequency Responses

Next the frequency responses are measured; x-directional response is shown in Fig. 24 while y-directional one is indicated in Fig. 25. They are measured using the FFT analyzer (MTS Siglab). In both cases the rigid mode is recognized about 150 [Hz] and the peak is well damped. Hence the controller can well stabilize the rotor.

G. Unbalance Responses

Unbalance responses are measured when the rotor is levitated rotating. The responses are shown in Fig. 26. The rotating speed is increased 200 [rpm] stepwise until stable rotation. Then the unbalance response is recorded using FFT analyzer (Ono Sokki, CF5220). The top speed of 3600 [rpm] is recorded. Over this speed the rotor touched down to the stator. This is considered due to the weak damping of the axial and tilt passive stability.

To improve the unbalance response with poor axial and tilt stability, the unbalance test is again carried out at the horizontal rotor position. The results are shown in Fig. 27. In this case the gravity is supported actively and the top speed reaches near the 8000 [rpm]. This is almost the same as radial resonance.

VI. Concluding Remarks

In this paper 4 pole 3 segmented Halbach magnet is applied to the outer rotor type Lorentz self-bearing motor. Halbach magnet has the merit of producing the strong sinusoidal flux density only one side. Previously proposed 8 pole motor does not have strong force and produces the levitation force fluctuation. Compared with 8 pole Halbach magnet one, the proposed 4 pole motor indicates stronger and stable levitated rotation. The top speed reaches

TABLE VII

CONTROL PARAMETERS

Parameter	Value
Proportional Gain K_p	15 [A/mm]
Derivative Gain K_d	0.069 [A· sec/mm]
Integral Gain K_i	70 [A/(sec· mm)]
Sampling Interval τ	0.1 [msec]
Derivative Time Constant T_d	0.8 [msec]

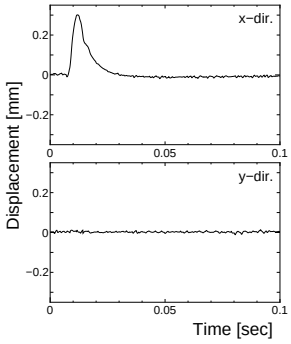

Fig. 22. Impulse Response (x direction hammering)

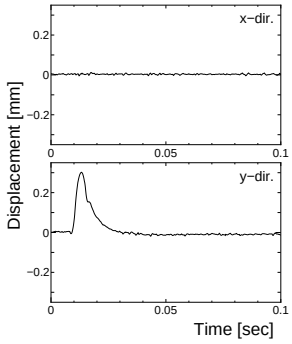

Fig. 23. Impulse Response (y direction hammering)

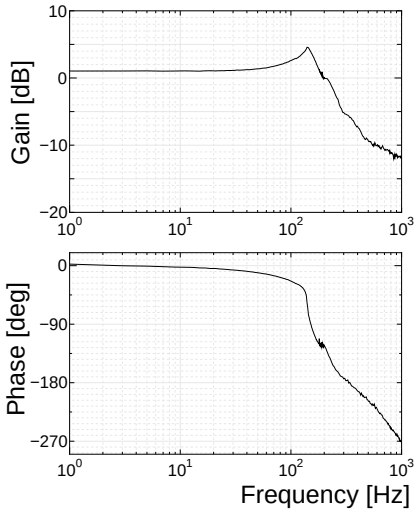

Fig. 24. Frequency Response (x direction)

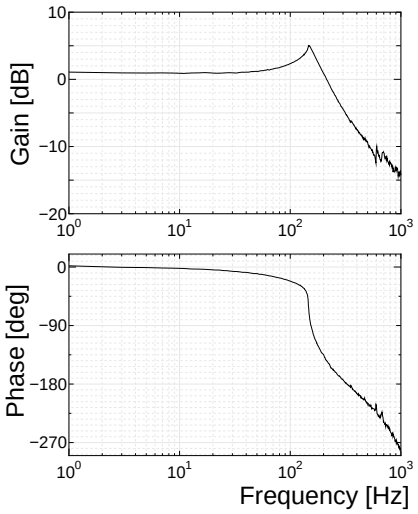

Fig. 25. Frequency Response (y direction)

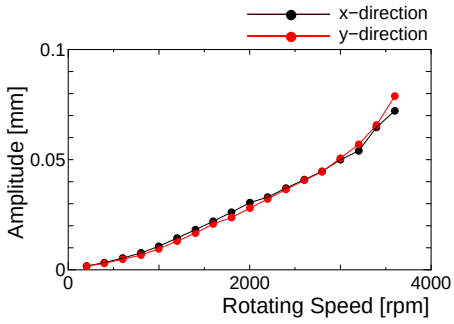

Fig. 26. Unbalance Response

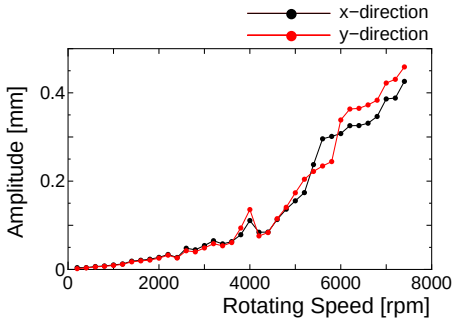

Fig. 27. Unbalance Response (Horizontal Position)

7400 [rpm] and the maximum efficiency is recorded as 72 [%]. However the 3 segmented PMs are very difficult for manufacturing. This is the only demerit of this type of self-bearing motor. Further work is continuing to apply this type motor to the implantable artificial heart pump or hard disc spindle.

Acknowledgement

The authors would thanks that the research is partly supported by the Grant-in Aid for Science Research (B)(1), under Project Number 13555059.

REFERENCES

[1] Y. Okada, et. al.: Fundamentals and Application of Magnetic Bearings, JSME publication series, Yokendo Ltd. Co., (1995), in Japanese (Korean translated book is available)

[2] A. Chiba, et al. : IEEE Trans. on Energy Conversion, Vol. 9, No. 1, 1994, pp. 61-67

[3] R. Schöb and N. Barletta : Proc. of 5th Int. Symp. on Magnetic Bearings, Kanazawa, Japan, August 28-30, 1996, pp. 313-318

[4] Y. Okada, et. al.: Lorentz Force type Self-Bearing Motor, Proc. of 6th Int. Symp. on Magnetic Bearings, ETH Zurich, Switzerland, August 23-25, 2000, pp. 353-358

[5] T. Tokumoto, et. al.: Development of Lorentz Force type Self-Bearing Motor, Proc. of 8th Int. Symp. on Magnetic Bearings, Mito, Japan, August 26-28, 2002, pp. 59-64

[6] D. Howe and Z. Q. Zhu : Proceedings of the Sixteenth International Workshop on Rare-Earth Magnets and Their Applications, The Japan Inst. of Metals, 2000, pp 903-922

[7] Y. Okada, et. al.: New Design of Lorentz Force type Self-Bearing Motor with Halbach Magnet, Proc. of 6th Korea-Japan Symp. of Frontiers in Vibration Science and Technology, Ibaraki University, Hitachi, Japan, July 14-15, 2005, pp. 1-6